

Video Article

# Generating a Murine Orthotopic Metastatic Breast Cancer Model and Performing Murine Radical Mastectomy

Eriko Katsuta<sup>1</sup>, Masanori Oshi<sup>1</sup>, Omar M. Rashid<sup>2,3,4,5</sup>, Kazuaki Takabe<sup>1,6,7,8,9,10</sup>

<sup>1</sup>Breast Surgery, Department of Surgical Oncology, Roswell Park Comprehensive Cancer Center

<sup>2</sup>Holy Cross Hospital Michael and Dianne Bienes Comprehensive Cancer Center

<sup>3</sup>Department of Surgery, Massachusetts General Hospital

<sup>4</sup>Department of Surgery, University of Miami Miller School of Medicine

<sup>5</sup>Department of Surgery, Nova Southeastern University School of Medicine

<sup>6</sup>Department of Surgery, University at Buffalo Jacobs School of Medicine and Biomedical Sciences

<sup>7</sup>Department of Breast Surgery and Oncology, Tokyo Medical University

<sup>8</sup>Department of Surgery, Yokohama City University

<sup>9</sup>Department of Surgery, Niigata University Graduate School of Medical and Dental Sciences

<sup>10</sup>Department of Surgery, Fukushima Medical University

Correspondence to: Eriko Katsuta at [Eriko.Katsuta@roswellpark.org](mailto:Eriko.Katsuta@roswellpark.org)

URL: <https://www.jove.com/video/57849>

DOI: [doi:10.3791/57849](https://doi.org/10.3791/57849)

Keywords: Medicine, Issue 141, Mouse, breast, cancer, model, orthotopic, syngeneic, mastectomy, metastasis, bioluminescence, IVIS

Date Published: 11/29/2018

Citation: Katsuta, E., Oshi, M., Rashid, O.M., Takabe, K. Generating a Murine Orthotopic Metastatic Breast Cancer Model and Performing Murine Radical Mastectomy. *J. Vis. Exp.* (141), e57849, doi:10.3791/57849 (2018).

## Abstract

In vivo mouse models to assess breast cancer progression are essential for cancer research, including preclinical drug developments. However, the majority of the practical and technical details are commonly omitted in published manuscripts which, therefore, makes it challenging to reproduce the models, particularly when it involves surgical techniques. Bioluminescence technology allows for the evaluation of small amounts of cancer cells even when a tumor is not palpable. Utilizing luciferase-expressing cancer cells, we establish a breast cancer orthotopic inoculation technique with a high tumorigenesis rate. Lung metastasis is assessed utilizing an *ex vivo* technique. We, then, establish a mastectomy model with a low local recurrence rate to assess the metastatic tumor burden. Herein, we describe, in detail, the surgical techniques of orthotopic implantation and mastectomy for breast cancer with a high tumorigenesis rate and low local recurrence rates, respectively, to improve breast cancer model efficiency.

## Video Link

The video component of this article can be found at <https://www.jove.com/video/57849/>

## Introduction

Animal models play a key role in cancer research. When a hypothesis is proven *in vitro*, it should be tested *in vivo* to evaluate its clinical relevance. Cancer progression and metastasis are often better captured by animal models as compared to *in vitro* models, and it is essential to test a new drug in an animal model as a preclinical study for drug development<sup>1,2</sup>. However, the technical details of animal experiments are often not well described in published articles, making it challenging to reproduce the model successfully. Indeed, the authors who established these orthotopic inoculation and mastectomy models went through long and rigorous processes of trial and error. The success rate of tumorigenesis after cancer cell inoculation is one of the key factors to determine the success and efficiency of an animal study<sup>3</sup>. The cell line and the number of cells to inoculate, the inoculation site, and the strain of the mice are all important factors. It is well known that there are huge variations in the results of animal experiments due to individual differences, compared to *in vitro* techniques. Therefore, using a well-established model with a standard technique is important to obtain stable results, to improve the efficiency of animal experiments, and to avoid misleading results.

This paper provides well-established techniques<sup>4</sup> to generate breast cancer orthotopic and mastectomy mouse models. The aims of these methods are 1) to mimic human breast cancer progression and treatment courses, and 2) to conduct *in vivo* experiments with greater efficiency and higher success rates compared to other breast cancer inoculation or mastectomy techniques. In orthotopic cancer cell inoculation, to mimic human breast cancer progression, we choose the #2 mammary fat pad as an inoculation site, which is located in the chest. In most of the studies, breast cancer cells are inoculated subcutaneously<sup>5</sup>. This technique does not require surgery and, thus, it is simple and straightforward. However, the subcutaneous microenvironment is quite different from the mammary gland microenvironment, which results in different cancer progression and even molecular profiles<sup>6,7</sup>. Some studies use the #4 mammary gland, which is located in the abdomen, as an inoculation site<sup>6</sup>. However, since #4 mammary glands are located in the abdomen, the most common metastatic pattern is peritoneal carcinomatosis<sup>7</sup>, which

occurs with less than 10% of metastatic breast cancer<sup>8</sup>. Breast cancer generated by the technique presented here, in the #2 mammary gland, metastasizes to the lung, which is one of the most common breast cancer metastatic sites<sup>9</sup>.

With this technique, the goal is also to achieve a higher tumorigenesis rate with minimal tumor size variability compared to other breast cancer inoculation techniques. To do so, cancer cells suspended in a gelatinous protein mixture are inoculated under direct vision through a median anterior chest wall incision. This technique produces a high tumorigenesis rate with less variability in tumor size and shape compared to subcutaneous or non-surgical injection, as previously reported<sup>3,7</sup>.

We also introduce a mouse radical mastectomy technique in which the orthotopic breast tumor is resected with the surrounding tissues and axillary lymph nodes. In the clinical setting, the standard of care for breast cancer patients without distant metastasis disease is mastectomy<sup>10,11</sup>. Before a mastectomy, axillary lymph node metastasis is surveyed by imaging and sentinel lymph node biopsy. If there is no evidence of axillary lymph node metastasis, the patient is then treated with a total or partial mastectomy, in which the axillary lymph node resection is omitted. Total mastectomy is a technique to resect breast cancer with the whole breast tissue en bloc, whereas partial mastectomy is to resect breast cancer with a margin of surrounding normal breast tissue only, thus conserving the remaining normal breast tissue in the patient. However, patients who preserve remaining normal breast tissue after a partial mastectomy require postoperative radiotherapy to avoid local recurrence<sup>10</sup>. Patients who have axillary lymph node metastasis undertake radical mastectomy which removes the breast cancer with all normal breast tissue and axillary lymph nodes and invaded tissues en bloc<sup>10,11</sup>. In the mouse model, surveillance for axillary lymph node metastasis and/or post-operative radiation is not reasonable or feasible. Thus, we utilize the radical mastectomy technique to avoid local or axillary lymph node metastasis.

Cancer cell inoculation via the tail vein is the most common lung metastasis mouse model<sup>12</sup>, the so-called "experimental metastasis". This model is easy to generate and does not require surgery; however, it does not mimic human breast cancer progression which may result in different metastatic disease behavior. In order to mimic the human breast cancer treatment course where metastasis often occurs after mastectomy, the primary tumor is removed after orthotopic cancer cell inoculation. This technique produces less local recurrence compared to simple tumor resection, as previously reported<sup>13</sup>, and is useful for novel therapeutics, preclinical studies, and for metastatic breast cancer research studies. The techniques described here are applicable for most breast cancer orthotopic model experiments. However, it is important to consider that the gelatinous protein mixture can affect the microenvironment and surgery can affect the stress/immune response<sup>14</sup>. Therefore, investigators studying the microenvironment and/or the stress/immune response should be aware of potential confounding factors.

## Protocol

Approval from the Roswell Park Comprehensive Cancer Center Institutional Animal Care and Use Committee was obtained for all experiments.

**NOTE:** Nine to twelve weeks-old female BALB/c mice are obtained. 4T1-luc2 cells, a mouse mammary adenocarcinoma cell line derived from BALB/c mice that has been engineered to express luciferase, are used. These cells are cultured in Roswell Park Memorial Institute (RPMI) 1640 medium with 10% fetal bovine serum (FBS).

## 1. Preparation of Instruments

1. Thaw a frozen gelatinous protein mixture (e.g., Matrigel) on ice in a tissue culture hood.
2. Clean and autoclave two sets of surgical instruments (microdissection scissors, Adson forceps, and a needle holder) prior to surgery. Prepare sterilized 5-0 silk sutures and dry sterilant (when serial surgeries are planned).
3. Clip the middle chest hair of the mice using a clipper and mark the mice for identification by punching the ear prior to the time of surgery.
4. **Prepare the procedure table, which can be immediately used for the operation.**
  1. Spread an absorbent pad and fix the corners with tape, fix anesthesia nose cones with tape, put sterilant and disinfectant (chlorhexidine, iodine, and 75% ethanol) beside the operating space, and place the mice in operation order.

## 2. Preparation of Cells (for 10 Mice)

**NOTE:** The cells should be inoculated within 1 h after being detached from the dish to avoid decreased cell viability. Specifically, the cell suspension should be mixed into the gelatinous protein mixture within 15 min after detaching the cells from the dish to maintain their viability.

1. Culture 4T1-luc2 cells, a mouse mammary adenocarcinoma cell line expressing luciferase, in RPMI 1640 media with 10% FBS in a humidified incubator at 37 °C in 5% CO<sub>2</sub>.
  2. Wash the adherent 4T1-luc2 cells in a 10-cm dish with phosphate-buffered saline (PBS) using a 10 mL serological pipette. Add 1 mL of 0.25% trypsin using a P1000 pipette and, then, incubate the sample at 37 °C for 5 min. Then, add 4 mL of growth media (RPMI-1640 with 10% FBS) using a 5 mL serological pipette and transfer the cell suspension to a 15-mL conical tube in a tissue culture hood. Centrifuge the cell suspension at 180 x g for 5 min.
  3. Aspirate the supernatant and resuspend the cells in 2 mL of PBS; then, count the cells using the hemocytometer.
  4. Suspend  $2 \times 10^6$  4T1-luc2 cells in 40  $\mu$ L of cold PBS (pH 7.4, 4 °C) in the tissue culture hood.
  5. Mix the 40- $\mu$ L cell suspension with 360  $\mu$ L of the gelatinous protein mixture in a 1.5 mL microcentrifuge tube on ice in the tissue culture hood.
- NOTE:** The final concentration is  $1 \times 10^5/20 \mu$ L (1:9 PBS:gelatinous protein mixture). For the orthotopic model (no mastectomy),  $1 \times 10^4/20 \mu$ L of the final concentration was used, to avoid reaching euthanasia criteria (tumor size > 2 cm) within two weeks.

## 3. Cancer Cell Inoculation

1. Put the mice in the anesthesia induction chamber with 2-4% isoflurane and 0.2 L/min oxygen flow until the mice breathe calmly (2–3 min).
2. Grasp the mouse and inject 0.05 mg/kg buprenorphine into its shoulder subcutaneously.

3. Confirm adequate anesthesia by the lack of reaction to a toe pinch. Insert the mouse's nose into the hole of the mouse mask, which allows inhalational anesthesia with 2-4% isoflurane and 2 L/min oxygen flow attached to a charcoal canister unit.
4. Restrain the mouse's limbs using lab tape and sterilize its skin using chlorhexidine, iodine, and 75% ethanol, using cotton swabs.
5. Make a 5 mm skin incision in the middle of the anterior chest wall utilizing sterile microdissection scissors, lift the right-side skin next to the incision and detach the skin from the chest wall using the scissors, and then, invert the skin to expose the right #2 mammary fat pad.
6. Carefully inject 20  $\mu$ L of cancer cell suspension using a 1 mL insulin syringe with a 28.5 G needle into the fat pad under direct vision through the wound.  
**NOTE:** The needle goes through the wound, not the skin. Keep holding the needle in the fat pad for 5 s prior to pulling it out, which allows time for the gelatinous protein mixture to solidify.
7. Close the skin incisions by stitching, using sterile 5-0 non-absorbable sutures.
8. After surgery, return the animals to a clean cage and monitor them until they have recovered and are moving freely (after ~1–2 min). If an animal does not appear to be in good health within 24 h of surgery, administer buprenorphine (0.2 mg/kg).
9. Remove the sutures under anesthesia (see step 3.1) 7 d after the surgery.

#### 4. Mastectomy

**NOTE:** The timing of the mastectomy is very important. If it is done too early, lung metastasis does not occur. If it is done too late, the primary tumor has invaded major blood vessels, which make a complete oncologic resection challenging. Thus, multiple time points were tested for mastectomy to determine which time point produced the appropriate balance in waiting for metastasis before resection became too challenging. After doing so in over 50 mouse experiments, it was demonstrated that mastectomy at 8 days after cancer cell inoculation (or when the tumor size reaches 5 mm) was the ideal time point to achieve that balance<sup>13</sup>.

1. Anesthetize a mouse with 2-4% inhaled isoflurane and inject buprenorphine (see steps 3.1 and 3.2).
2. Restrain the mouse and sterilize its skin (see step 3.4).
3. Make a 5 mm skin incision 2 mm to the left from the surgical scar that was made at the initial cancer cell inoculation, using the microdissection scissors. Extend the incision toward the root of the forelimb to remove the tumor, the skin including the surgical scar, and the lesion in contact with the tumor, as well as the axillary lymph node basin in which most of the time no visible lymph node exists at the time of the mastectomy<sup>13</sup>. Make sure not to damage the axillary vein.
4. Close the skin defects by stitching, using sterile 5-0 non-absorbable sutures in the shape of a "Y".
5. The same as in step 3.8, return the mouse to a clean cage and monitor until they have recovered.
6. Remove the sutures under anesthesia (see step 3.1) 7 days after surgery.

#### 5. Bioluminescent Quantification of the Primary Tumor (Orthotopic Inoculation Without Mastectomy) or Lung Metastasis (Mastectomy Model)

**NOTE:** For primary tumor burden quantification, the bioluminescence is measured 2x a week from the day after the orthotopic inoculation. For lung metastasis quantification, the bioluminescence is measured 2x a week from the day after the mastectomy.

1. Dissolve D-luciferin in Dulbecco's phosphate-buffered saline (DPBS) to a final concentration of 15 mg/mL in a tissue culture hood. Aliquot it into light-shielded 1.5 mL microcentrifuge tubes. Store the diluted solution at -80 °C.  
**NOTE:** For a 20 g mouse, 200  $\mu$ L of diluted D-luciferin is required.
2. Open the imaging software and click **Initialize**.  
**NOTE:** It takes about 15 min to cool the charge-coupled device (CCD). When the CCD reaches the set temperature, the color of the **Temperature** bar changes from red to green.
3. Anesthetize the mice with 2-4% isoflurane in a dedicated induction chamber prior to imaging (see step 3.1).
4. Weigh the mice.
5. Inject 150 mg/kg D-luciferin intraperitoneally at the point of the mid-abdomen, using a 28.5 G needle.
6. Fit each mouse with a nose cone inside the imaging system in the supine position (place a maximum of five mice at the same time). Maintain anesthesia at 1% - 3% isoflurane (in 100% oxygen) through the nose cones during imaging.
7. **Capture an image every 5 min to detect the peak bioluminescence for 50 min (or up to the confirmed peak bioluminescence).**
  1. Select **Luminescence** as **Auto**, **Binning** as **Medium**, and **Field of View** as **D**.
  2. Click **Acquire** to capture the image.
8. Return the mice to their cage(s) and monitor them until they have recovered (see step 3.8).

#### 6. Lung Metastasis Tumor Burden Quantification by Ex Vivo Imaging

**NOTE:** Lung metastasis quantification is applicable for orthotopic inoculation both with and without mastectomy models. In the mastectomy model, ex vivo imaging or survival observation is chosen, depending on the purpose. In the orthotopic inoculation (without mastectomy) model, most cases produce primary tumor size euthanasia criteria (> 2 cm) approximately 21 days after inoculation.

1. Quantify lung metastatic lesions 21 days after the cancer cell inoculation by ex vivo imaging.
2. Anesthetize the mice with 2-4% isoflurane in a dedicated induction chamber (see step 3.1).
3. Weigh the mice.
4. Inject 150 mg/kg D-luciferin intraperitoneally (see step 5.6).
5. Euthanize the mice by cervical dislocation, 15 min after the injections.
6. Open the abdomen by cutting the skin and peritoneum at the mid-abdomen, using curved Mayo scissors. Extend the incision to both the right and the left. Pull out the liver with forceps until the diaphragm is visualized; then, cut the diaphragm.

7. Using the curved Mayo scissors, cut the bilateral ribs from caudad (12th ribs) to cephalad (1st ribs) to expose the lungs by flipping the anterior thorax wall.
8. Identify the thoracic esophagus, which looks like a cord connecting the lungs to the spine, by lifting the lungs using forceps and, then, cut the esophagus using the microdissection scissors.
9. Lift the bilateral lungs and heart using forceps (applying traction pulling down, in the direction of cephalad to caudad) and, then, cut the trachea and major vessels to the lung apex at the cephalad, using microdissection scissors.  
**NOTE:** This allows for the isolation of the lung and heart from the body.
10. Remove the heart from the lung using microdissection scissors.
11. Put the lungs in a 10 cm Petri dish.
12. Capture the bioluminescence image (see steps 5.7.1 and 5.7.2) 5 min after euthanasia (20 min after the luciferin injection).

## Representative Results

The purpose of the orthotopic model is to mimic human cancer progression (*i.e.*, the growth of the primary tumor followed by lymph node metastasis and then distant lung metastasis)<sup>15</sup>. After cancer cell inoculation, the bioluminescence is quantified regularly (two to three times/week) (**Figure 1A**). The bioluminescence in the lungs is deeper and smaller than the primary lesion. The bioluminescence mainly reflects the primary tumor burden in live mice<sup>3</sup> (**Figure 1B and 1C**). The tumor size was also measured by caliper measurement. The tumor volume was estimated using the following equation: volume = (length) x (width)<sup>2</sup>/2 (**Figure 1D**). Quantification of the tumor burden by bioluminescence and caliper measurement showed similar trends in the representative results (**Figure 1B and 1D**); however, we sometimes encountered discrepancies. We assume that quantifying the primary tumor burden utilizing bioluminescence is more accurate compared to measuring the tumor size by caliper when the tumor size is less than 1.5 cm. Because it reflects viable cancer cells, even a small number of cells can be detected by bioluminescence, and only cancer cells can be detected inside of the tumor, not including infiltrating immune cells or surrounding stromal cells<sup>3</sup>. This model is useful in evaluating the efficacy of tumor regression mediated by anti-cancer drug and immune responses<sup>3,7,16</sup>. The tumor burden of the lung metastases can also be quantified by *ex vivo* imaging in this model (**Figure 1E**); however, the limitation is that the mice must be euthanized to quantify the metastatic tumor burden.

The purpose of the mastectomy model is to 1) reproduce the standard of care treatment of human breast cancer, which is the surgical removal of the primary tumor<sup>17</sup>, and 2) allow the serial quantification of the metastatic tumor burden *in vivo*. This model is particularly useful in the preclinical study of the development of novel therapeutics<sup>13</sup>. As previously published, an Src inhibitor, AZD0530, which showed efficacy in the preclinical mice model but failed in a clinical trial for breast cancer treatment, showed efficacy in the primary lesion utilizing orthotopic inoculation without mastectomy but not in lung metastasis utilizing the mastectomy model presented here. Although anti-cancer drugs (*e.g.*, anthracyclines) are sometimes used in humans as neoadjuvant therapy to treat primary breast tumors, the vast majority of drugs are used as adjuvant therapy where drugs are given after surgery to reduce the risk of recurrence by treating clinically undetectable cancer or as palliative treatment for metastatic cancer<sup>1,7,18</sup>. Thus, this mastectomy model was established, which mimics the human treatment process<sup>11</sup>.

Eight days after the cancer cell inoculation, the primary tumor is surgically removed (**Figure 2**). To test any of the drug efficacies for metastatic lesions, it should be administrated after the mastectomy. This model allows for lung metastatic lesion quantification, as well as whole-body metastatic lesion quantification, as long as the metastatic tumor burden has a detectable bioluminescence utilizing *in vivo* imaging. The anterior chest wall local recurrence rate is quite low. In our experience, the local recurrence rate was less than 5% in over 50 mice experiments. However, if the postoperative day 1 bioluminescence exceeds 1.00E + 06 photons (10x larger than other individuals), there is a high possibility of a local residual tumor<sup>13</sup>. If there are remnant cancer cells present, a palpable tumor appears within two weeks. When there is a local residual tumor, the bioluminescence mainly reflects that local recurrence rather than any metastatic lesions. Local residual tumors are known to behave very differently than distant metastases<sup>19</sup>; thus, those animals with local recurrence (<5% in our experience) should be excluded from any further analysis. This mastectomy model also allows for serial metastatic tumor burden monitoring without having to euthanize the animals. Furthermore, such bioluminescent monitoring can be confirmed by *ex vivo* lung metastasis quantification. Instead of quantifying lung metastases by *ex vivo* imaging, thus having to euthanize the animals, mice survival after surgical treatment can also be monitored as a translatable clinical endpoint (**Figure 2D**). Since there is no primary lesion, mice cannot meet euthanasia tumor criteria which are generally defined as a tumor size of >2 cm or ulceration of the primary tumor. In this 4T1 mastectomy model, all mice died within 60 days after cancer cell inoculation due to metastasis.

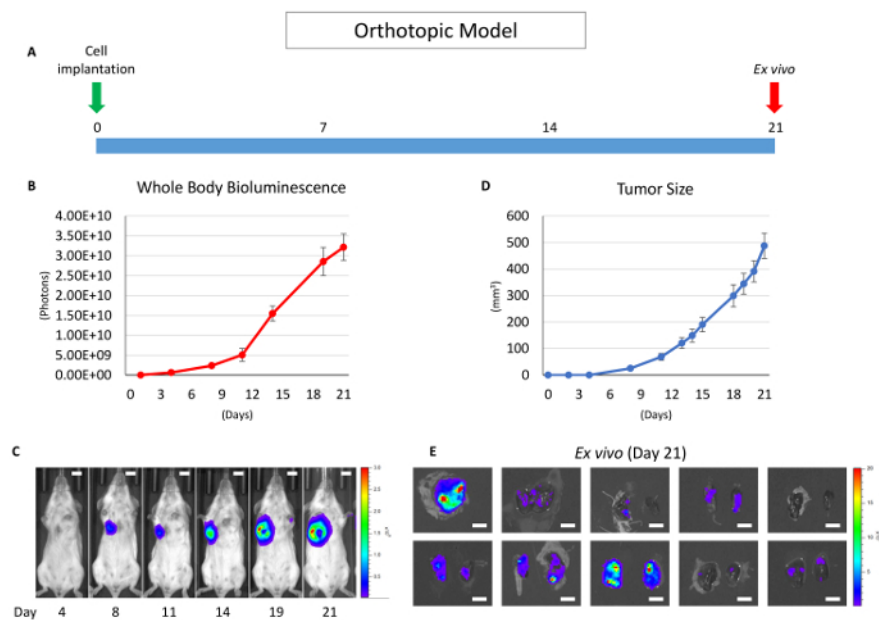


**Figure 1: Overview of the orthotopic model without mastectomy.** (A) This panel shows a time course of the orthotopic model utilizing the 4T1 syngeneic model. (B) This panel shows the whole-body bioluminescence of an orthotopic model which mainly reflects the primary tumor. The error bar indicates the standard error of the mean ( $n = 10$ ). (C) This panel shows serial images of whole-body bioluminescence (of the same mouse). The scale bar indicates 1 cm. (D) This panel shows the actual tumor size of panel B, measured by calipers. The error bar indicates the standard error of the mean ( $n = 10$ ). (E) This panel shows lung ex vivo bioluminescence images of 10 orthotopic model mice ( $n = 10$ ). The scale bar indicates 1 cm. [Please click here to view a larger version of this figure.](#)

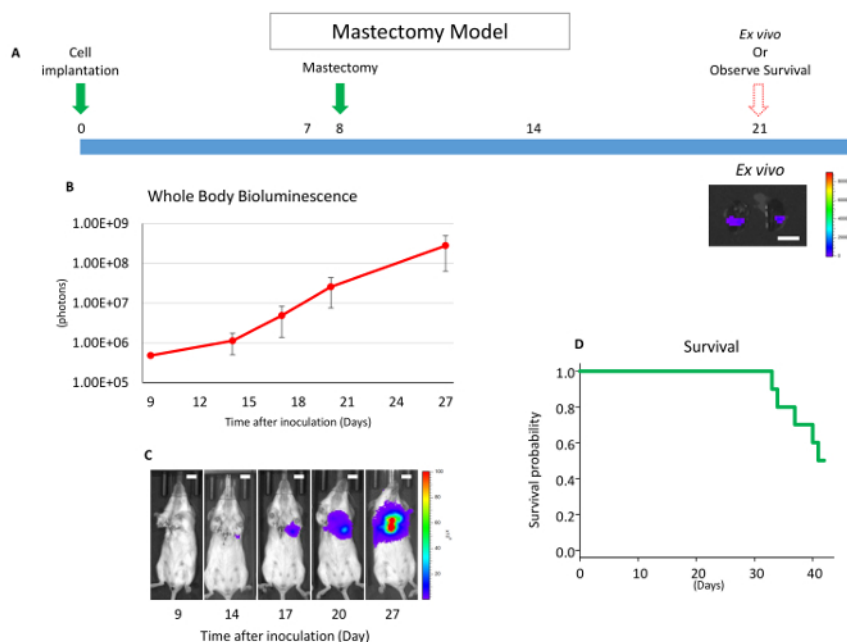


**Figure 2: Overview of the mastectomy model.** (A) This panel shows a time course of the mastectomy model after 4T1 orthotopic syngeneic implantation. The scale bar indicates 1 cm. (B) This panel shows the whole-body bioluminescence of the mastectomy model, which mainly reflects metastatic lesion. The error bar indicates the standard error of the mean ( $n = 10$ ). (C) This panel shows serial images of whole-body bioluminescence (of the same mouse). Utilizing ex vivo imaging, it was confirmed that the signals were from lung metastasis, and no local recurrence was confirmed by whole-body imaging after lung removal. Scale bar = 1 cm. (D) This panel shows the Kaplan-Meier survival curve of the mastectomy model without any drug treatment. Mice were euthanized when they reached euthanasia criteria with any morbid condition. [Please click here to view a larger version of this figure.](#)



## Discussion

For the last decade, we have been establishing multiple murine cancer models, including breast cancer models<sup>3,7,13,16,20,21</sup>. Previously, we demonstrated that breast cancer cell orthotopic inoculation into the mammary gland tissue under direct vision produced a larger tumor with less size variability compared to injecting cells around the nipple without a surgical incision<sup>7</sup>. This model has been improved upon by utilizing a cell suspension in a gelatinous protein mixture. The shapes of the tumor generated by the gelatinous protein mixture-suspended cells were round with less variability, whereas those generated by PBS-suspended cells were scattered in the mammary gland<sup>3</sup>.

We further verified that the tumors generated by the surgical orthotopic implantation method presented here highly expressed the genes whose interaction networks are important in cancer progression compared to those generated by non-surgical or subcutaneous injection<sup>7</sup>. These findings imply that this model mimics human breast cancer better compared to non-surgical orthotopic or subcutaneous implantation<sup>7</sup>. We also demonstrated that this model is suitable to evaluate the immune-mediated regression of breast cancer using allogeneic rejection<sup>3</sup>. However, skin incision can also cause inflammation around the tumor<sup>14</sup>. Therefore, depending on the hypothesis tested by the investigator, it is important to consider inflammation as a possible confounding factor.

Other than the neoadjuvant setting, the vast majority of systemic therapies are administered after the primary breast tumor is surgically removed<sup>11</sup>. To date, the majority of preclinical studies for new drug development evaluate drug response in the primary tumor, but not in the metastatic lesions<sup>1,18</sup>. This discrepancy between animal models and human treatment is important because the gene profile of the metastatic lesions is significantly different from those of the primary lesion<sup>22</sup>, which has important implications for cancer biology and treatment, especially in the era of targeted therapy<sup>22</sup>. Therefore, the efficacy of the drug for adjuvant therapy should be evaluated in the metastatic lesions, not merely in the primary tumor. We verified the timing of the lymph node and lung metastasis formation after orthotopic inoculation, utilizing the 4T1 breast cancer orthotopic model<sup>16</sup>. We also demonstrated that a resection of the primary tumor improved survival in the metastatic breast cancer utilizing the mastectomy model<sup>23</sup>. Thus, we tried to establish a mastectomy model after orthotopic cancer cell implantation. However, a long time was spent to establish this low local recurrence model. Because cancer cells are injected through surgical incision, cancer cells easily migrate into the wound. In addition, cancer cells invade tissues in direct contact with the tumor, such as the surrounding chest wall muscle and skin. The cancer cells also metastasize to axillary lymph nodes without forming a visible axillary mass at the time of the mastectomy. While removing the tumor may be an easier technique, doing so is not translatable to mastectomy in breast cancer treatment as it causes local recurrence<sup>13</sup>. Thus, this "radical mastectomy model" was established in order to remove all cancer cells from the anterior chest wall and axillary lymph node basin, as described in **Figure 2**. We confirmed lung metastasis by histology and lung ex vivo imaging, and there was no shining lesion present by whole-body imaging after lung removal. In this 4T1 orthotopic model, cancer cells eventually metastasize to the lungs, in all cases within 21 days. However, the timing of metastasis depends on the primary tumor size; thus, less primary tumor size variability is important for monitoring not only the primary tumor but also the metastatic tumor burden. By using the gelatinous protein mixture, tumor size variability can be minimized. However, the gelatinous protein mixture can also affect the tumor microenvironment. Therefore, the potential confounding factors associated with gelatinous protein mixture use should be considered, depending on the hypothesis of the investigator.

Utilizing these techniques and luciferase-expressing cancer cells allow for tumor burden quantification with less measurement error, even in non-palpable tumors. There are two reporter systems, bioluminescent and fluorescent, to visualize the signals in live animals. While it has been reported that the signal of both bioluminescence and fluorescence can be bright enough for quantification, when the target signal is very low, the background signal of fluorescence is higher, which reduces the accuracy of the assay. In contrast, bioluminescence is detected with greater accuracy at a lower signal with less background interference<sup>24</sup>. Accordingly, most investigators prefer to use bioluminescence reporter systems in live animal experiments<sup>24,25</sup>. However, tumor burden quantification by bioluminescence has its limitations. Luciferase-expressing cells shine when luciferin reaches the cancer cells by cardiovascular perfusion<sup>26</sup>. If the lesion has an area of hypoxia and/or hypoperfusion, luciferin is not delivered to the cells and the bioluminescence value could, then, be measured to be lower than the actual tumor burden. Indeed, we have experienced inappropriate bioluminescence quantification when the tumor size reached more than 1.5 cm. We assume that it is due to the described hypoxic and/or hypoperfused condition. Thus, when the tumor reaches a palpable size, the tumor burden is quantified by both bioluminescence and caliper measurement. An important limitation of bioluminescence quantification to consider is the black fur of mice. Even after the fur is removed, there is pigmentation on the skin<sup>27</sup>. While bioluminescence can be detected and quantified in mice with black fur, it is decreased and, therefore, it is important to compare mice of the same fur color to each other in order to reduce the confounding effects of fur color on bioluminescent quantification. The use of luciferase-expressing cells provides some unique modalities for study. For example, secreted luciferase can be used for tumor burden quantification by measuring blood or urine bioluminescence<sup>28</sup>. In the model presented here, direct tumor burden quantification of viable cancer cells in live animals with non-secreted luciferase is simple and straightforward, which does not require collecting blood or urine samples.

Similar to the models which introduced here, the production of a more efficient animal experiment by producing a higher success rate of tumorigenesis with less variability is key to prove the findings. In the present model, once an investigator has learned the technique, it is easy to achieve a 100% tumorigenesis rate. We also achieved higher tumorigenesis rates other than the models we have introduced; plus, we have established a colon cancer orthotopic model utilizing cell suspension in a gelatinous protein mixture, together with bioluminescence technology to quantify the tumor burden<sup>21</sup>. In conclusion, the animal model presented here provides a suitable murine model to conduct cancer study.

## Disclosures

The authors have nothing to disclose.

## Acknowledgements

This work was supported by NIH grant R01CA160688 and Susan G. Komen Foundation Investigator Initiated Research grant (IIR12222224) to K.T. Mice bioluminescence images were acquired by shared resource Translational Imaging Shared Resource at Roswell Park Comprehensive Cancer Center, which was supported by the Cancer Center Support Grant (P30CA01656) and Shared Instrumentation grant (S10OD016450).

## References

1. Rashid, O. M., Takabe, K. Animal models for exploring the pharmacokinetics of breast cancer therapies. *Expert Opinion on Drug Metabolism & Toxicology*. **11** (2), 221-230 (2015).
2. Schuh, J. C. Trials, tribulations, and trends in tumor modeling in mice. *Toxicologic Pathology*. **32** Suppl 1, 53-66 (2004).
3. Katsuta, E. *et al.* Modified breast cancer model for preclinical immunotherapy studies. *Journal of Surgical Research*. **204** (2), 467-474 (2016).
4. Sidell, D. R. *et al.* Composite mandibulectomy: a novel animal model. *Otolaryngology-Head and Neck Surgery*. **146** (6), 932-937 (2012).
5. Ewens, A., Mihich, E., Ehrke, M. J. Distant metastasis from subcutaneously grown E0771 medullary breast adenocarcinoma. *Anticancer Research*. **25** (6b), 3905-3915 (2005).
6. Kocaturk, B., Versteeg, H. H. Orthotopic injection of breast cancer cells into the mammary fat pad of mice to study tumor growth. *Journal of Visualized Experiments*. (96), e51967 (2015).
7. Rashid, O. M. *et al.* An improved syngeneic orthotopic murine model of human breast cancer progression. *Breast Cancer Research and Treatment*. **147** (3), 501-512 (2014).
8. Bertozzi, S. *et al.* Prevalence, risk factors, and prognosis of peritoneal metastasis from breast cancer. *SpringerPlus*. **4**, 688 (2015).
9. Kennecke, H. *et al.* Metastatic behavior of breast cancer subtypes. *Journal of Clinical Oncology*. **28** (20), 3271-3277 (2010).
10. Valero, M. G., Golshan, M. Management of the Axilla in Early Breast Cancer. *Cancer Treatment and Research*. **173**, 39-52 (2018).
11. National Comprehensive Cancer Network. *Breast Cancer, NCCN Clinical Practice Guidelines in Oncology*. [https://www.nccn.org/professionals/physician\\_gls/pdf/breast.pdf](https://www.nccn.org/professionals/physician_gls/pdf/breast.pdf) (2018).
12. Versteeg, H. H. *et al.* Inhibition of tissue factor signaling suppresses tumor growth. *Blood*. **111** (1), 190-199 (2008).
13. Katsuta, E., Rashid, O. M., Takabe, K. Murine breast cancer mastectomy model that predicts patient outcomes for drug development. *Journal of Surgical Research*. **219**, 310-318 (2017).
14. Veenhof, A. A. *et al.* Surgical stress response and postoperative immune function after laparoscopy or open surgery with fast track or standard perioperative care: a randomized trial. *Annals of Surgery*. **255** (2), 216-221 (2012).
15. Wei, S., Siegal, G. P. Surviving at a distant site: The organotropism of metastatic breast cancer. *Seminars in Diagnostic Pathology*. **35** (2), 108-111 (2018).
16. Nagahashi, M. *et al.* Sphingosine-1-phosphate produced by sphingosine kinase 1 promotes breast cancer progression by stimulating angiogenesis and lymphangiogenesis. *Cancer Research*. **72** (3), 726-735 (2012).
17. Jones, C., Lancaster, R. Evolution of Operative Technique for Mastectomy. *Surgical Clinics of North America*. **98** (4), 835-844 (2018).
18. Rashid, O. M., Maurente, D., Takabe, K. A Systematic Approach to Preclinical Trials in Metastatic Breast Cancer. *Chemotherapy* (Los Angeles). **5** (3) (2016).
19. Ramaswamy, S., Ross, K. N., Lander, E. S., Golub, T. R. A molecular signature of metastasis in primary solid tumors. *Nature Genetics*. **33** (1), 49-54 (2003).
20. Aoki, H. *et al.* Murine model of long-term obstructive jaundice. *Journal of Surgical Research*. **206** (1), 118-125 (2016).
21. Terracina, K. P. *et al.* Development of a metastatic murine colon cancer model. *Journal of Surgical Research*. **199** (1), 106-114 (2015).
22. Rashid, O. M. *et al.* Is tail vein injection a relevant breast cancer lung metastasis model? *Journal of Thoracic Disease*. **5** (4), 385-392 (2013).
23. Rashid, O. M. *et al.* Resection of the primary tumor improves survival in metastatic breast cancer by reducing overall tumor burden. *Surgery*. **153** (6), 771-778 (2013).
24. Troy, T., Jekic-McMullen, D., Sambucetti, L., Rice, B. Quantitative comparison of the sensitivity of detection of fluorescent and bioluminescent reporters in animal models. *Molecular Imaging*. **3** (1), 9-23 (2004).
25. Adams Jr., S. T., Miller, S. C. Beyond D-luciferin: expanding the scope of bioluminescence imaging *in vivo*. *Current Opinion in Chemical Biology*. **21**, 112-120 (2014).
26. Close, D. M., Xu, T., Sayler, G. S., Ripp, S. In vivo bioluminescent imaging (BLI): noninvasive visualization and interrogation of biological processes in living animals. *Sensors* (Basel). **11** (1), 180-206 (2011).
27. Chen, H., Thorne, S. H. Practical Methods for Molecular In Vivo Optical Imaging. *Current Protocols in Cytometry*. **59** (1224) (2012).
28. Wurdinger, T. *et al.* A secreted luciferase for ex vivo monitoring of *in vivo* processes. *Nature Methods*. **5** (2), 171-173 (2008).
29. Aoki, H. *et al.* Host sphingosine kinase 1 worsens pancreatic cancer peritoneal carcinomatosis. *Journal of Surgical Research*. **205** (2), 510-517 (2016).